Evaluation of bone deformities of the femur, tibia, and patella in Toy Poodles with medial patellar luxation using computed tomography

Shinji Yasukawa[1]; Kazuya Edamura[1]; Koji Tanegashima[1]; Mamiko Seki[1]; Kenji Teshima[1]; Kazushi Asano[1]; Tomohiro Nakayama[2]; Kei Hayashi[3]

[1]Laboratory of Veterinary Surgery, Department of Veterinary Medicine, College of Bioresource and Sciences, Nihon University, Fujisawa, Kanagawa, Japan; [2]Laboratory of Veterinary Radiology, Department of Veterinary Medicine, College of Bioresource and Sciences, Nihon University, Fujisawa, Kanagawa, Japan; [3]Department of Clinical Sciences, College of Veterinary Medicine, Cornell University, Ithaca, NY, USA

Keywords

Computed tomography, deformity, dog, patellar luxation, radiography

Summary

Objectives: To evaluate morphological parameters of the femur, tibia, and patella in Toy Poodles with medial patellar luxation (MPL) using three-dimensional (3D) computed tomography (CT) and to compare these parameters between radiography and CT.

Methods: Thirty-five hindlimbs of Toy Poodles were divided into normal and grade 2 and 4 MPL groups. The anatomical and mechanical lateral proximal femoral angle, anatomical and mechanical lateral distal femoral angle (aLDFA, mLDFA), femoral varus angle (FVA), inclination of the femoral head angle, procurvation angle, anteversion angle (AA), frontal angle of the femoral neck, mechanical medial proximal or distal tibial angle, mechanical cranial proximal or distal tibial angle, tibial plateau angle, tibial torsion angle (TTA), Z angle, relative tibial tuberosity width, ratio of the medial distance of tibial tuberosity to the proximal tibial width (MDTT/PTW), patella size, and the patellar ligament length: patellar length (L:P) ratio were evaluated on radiography and 3D CT.

Results: The aLDFA, mLDFA, FVA, and TTA were significantly larger and the AA, MDTT/PTW, and patella were significantly smaller in the grade 4 MPL group. There were significant differences in many parameters between imaging tools, and CT was considered less susceptible to potential artefacts and rotational deformities.

Clinical significance: Toy Poodles with grade 4 MPL had significant femoral varus deformity, medial displacement of the tibial tuberosity, internal torsion of the proximal tibia, and hypoplasia of the patella.

Correspondence to:
Kazuya Edamura, PhD, DVM, Diplomate JCVS
Laboratory of Veterinary Surgery
Department of Veterinary Medicine
College of Bioresource Sciences, Nihon University
1866 Kameino, Fujisawa, Kanagawa 252–0880
Japan
Phone: +81 466 84 3389
Fax: +81 466 84 3389
E-mail: edamura.kazuya@nihon-u.ac.jp

Vet Comp Orthop Traumatol 2016; 29: 29–38
http://dx.doi.org/10.3415/VCOT-15-05-0089
Received: May 29, 2015
Accepted: October 13, 2015
Epub ahead of print: December 7, 2015

Introduction

Medial patellar luxation (MPL) is one of the most common orthopaedic diseases affecting the hindlimbs in dogs (1–3). Most cases of canine MPL are regarded as being congenital or developmental in original because they occur at birth or early in life without trauma (3). A predisposition to MPL has been reported in small breeds including the Pomeranian, Yorkshire Terrier, Toy Poodle, Chihuahua, Papillon, and Maltese (3–8). A heritable basis for MPL has been suspected in dogs (6–9).

Medial patellar luxation, depending on its severity, can lead to a varying degree of bone deformity of both the femur and tibia. Bone deformities that have been reported in association with MPL include coxa vara, varus deformity of the distal one-third of the femur, external torsion of the distal femur, shallow trochlear sulcus with poorly developed or absent medial ridge, hypoplasia of the medial condyle, medial displacement of the tibial tuberosity associated with internal torsion of the proximal tibia, and valgus deformity of the proximal tibia (1, 3, 10). Traditionally, these bone deformities have been evaluated using radiographs. Radiography is one of the most commonly used imaging tools in the small-animal practice. However, radiographs are two-dimensional images of three-dimensional structures, and the measurements are affected by positioning. In dogs with severe MPL, some measurements cannot be obtained because of difficulty in obtaining an ideal radiographic position. Therefore, there are limitations to accurate evaluation of bone morphology by plain radiography (11). In contrast, computed tomography (CT) can evaluate three-dimensional (3D) bone morphology, and should enable a more accurate assessment of bone deformities.

To the best of our knowledge, only radiography has been used in most previous studies evaluating bone morphology in dogs with MPL. In addition, measurements in those studies were not comprehensive, as most of them evaluated only the femur (9, 11–14). In severe MPL, multiple bone deformities can occur in the femur, tibia, and patella, and we have found only a few reports that have evaluated both the femur and tibia in dogs with MPL by radiography (15, 16). Computed tomography can more accurately evaluate bone deformities associated with canine MPL (15, 17, 18). A comprehensive evaluation of bone deformities associated with MPL in the femur, tibia, and patella using CT may contribute to a much better understanding of the pathophysiology of MPL in dogs and can be expected to help determine treatment strategies for MPL.

The purposes of this study were to comprehensively measure by CT the values for the femur, tibia, and patella that have been previously reported in radiographic studies, to compare the resulting morphological findings with the severity of MPL, and to compare the resulting morphological findings between radiography and CT in the Toy Poodle.

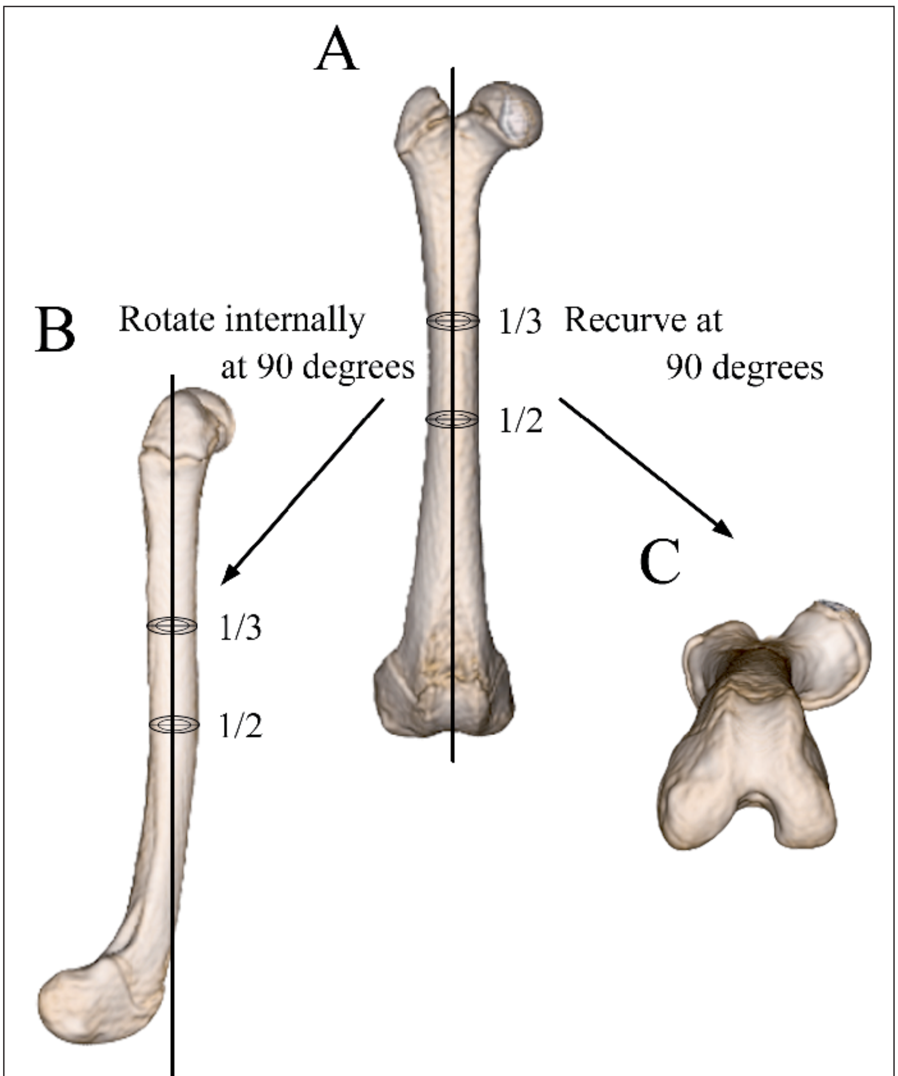

Figure 1 Frontal, lateral, and axial views of the femur on three-dimensional computed tomography. **A)** Frontal view of the femur. The view is determined as the plane tangent to the cranial flat cortex on the transverse plane that includes the lesser trochanter and is perpendicular to the reference line. **B)** Lateral view of the femur. The view is obtained as the frontal view of the femur is rotated internally at 90 degrees, centring around the reference line. **C)** Axial view of the femur. The view is obtained as the frontal view of the femur is recurved at 90 degrees on the sagittal plane. Black line: reference line of the femur.

Materials and methods

Patients

We prospectively evaluated the hindlimbs of Toy Poodles that were presented to the Animal Medical Center at Nihon University (Kanagawa, Japan) between April 2012 and October 2014 and were diagnosed by palpation as suffering from MPL. This study was conducted with the approval of the director of the hospital, and all owners of dogs used in this study consented to the collection of data. Radiography and CT were performed in all hindlimbs evaluated in this study. The hindlimbs with MPL were classified according to the Singleton grading system, and grades 2 and 4 were included in the analysis (19). Hindlimbs of dogs without orthopaedic disease other than MPL were employed as controls. All measurement values from radiography and CT were obtained using a PACS workstation[a].

Radiography

All radiographs were obtained using a computed radiography system[b]. Craniocaudal and mediolateral views of each femur or tibia were obtained separately. For the craniocaudal view of the femur, dogs were positioned in dorsal recumbency with the hip joints extended and the femurs parallel to the radiographic table (20). We confirmed appropriate positioning as follows: patella in the centre of the trochlear sulcus, bi-

a Osirix, Osirix Foundation, Lausanne, Switzerland
b FCR XG-1V Computed Radiography, Fujifilm Co., Ltd., Kanagawa, Japan

section of each fabella by the respective femoral cortex, and protrusion of the corticocancellous tip of the lesser trochanter from the medial aspect of the femur (20). For the mediolateral view of the femur, the dogs were positioned in lateral recumbency with the lowermost limb being the one under investigation. The femur was held parallel to the radiographic table with the femoral condyles superimposed in a neutral position (21). For the craniocaudal view of the tibia, the tibia was positioned such that the medial aspect of the calcaneus was aligned with the base of the sulcus of the talus (22). Mediolateral radiographs of the entire tibia, stifle, and tarsus were obtained with the tibia parallel to the radiographic table and the beam centred on the mid-tibial diaphysis in a neutral position (23).

Computed tomography

All CT images were acquired in a 16-slice helical scanner[c] and were reconstructed as 3D images using image processing software[d]. Dogs were positioned in dorsal recumbency with both the hip and stifle joints flexed at approximately 90 degrees. Images were obtained with a slice thickness of 0.5 mm and reconstruction intervals of 0.3 mm.

The reference line of the femur was drawn through two landmarks that were determined as each being the centre of the concentric circles at the proximal one-third and one-half length of the femur on the transverse planes (▶Figure 1A). The frontal, lateral, and axial views of the femur were then obtained using this reference line (▶Figure 1).

The reference line of the tibia was drawn connecting two landmarks. The proximal landmark was determined as the mid-point of the medial and lateral intercondylar eminences (▶Figure 2A, B) (23). The distal landmark was determined as the centre of the trochlea of the talus by identifying the centre of the concentric circle created by the trochlea of the talus on the lateral plane together with the sagittal plane passing through the bottom of the trochlea of the talus (▶Figure 2A, B) (23). Then, frontal and lateral views of the tibia were obtained using this reference line (▶Figure 2). In addition, to accurately evaluate the morphology of the proximal tibia even when internal torsion of the proximal tibia was severe, a proximal lateral view was obtained (▶Figure 2C). Based on previous studies, proximal and distal transverse CT slices of the tibia were obtained to evaluate tibial torsion (22, 24). Furthermore, an axial view of the tibia was acquired to evaluate the medial displacement of the tibial tuberosity (▶Figure 2D).

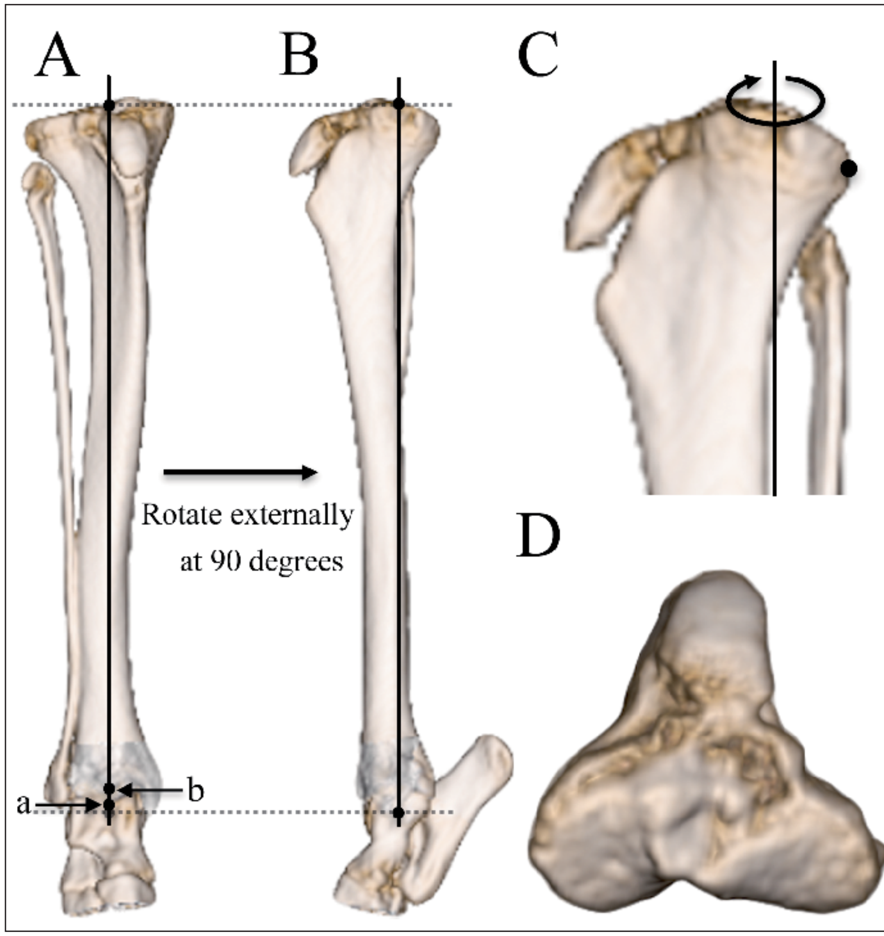

Figure 2 Frontal, lateral, proximal lateral, and axial views of the tibia on three-dimensional computed tomography. **A)** Frontal view of the tibia. The view aligns the most distal aspects of the cranial (a) and caudal cortices (b) of the tibia on the sagittal plane passing through the bottom of the trochlea of the talus in the reference line. **B)** Lateral view of the tibia. The view is obtained as the frontal view of the tibia is rotated externally at 90 degrees, centring around the reference line. **C)** Proximal lateral view of the tibia. The view is obtained by superimposing the caudal edge of each medial and lateral tibial condyle, with centring around the reference line. **D)** Axial view of the tibia. The view is determined as the plane passing through the tibial tuberosity and each caudal edge of the medial and lateral condyle. Black line: reference line of the tibia.

Femur

The anatomical lateral proximal femoral angle (aLPFA), mechanical lateral proximal femoral angle (mLPFA), anatomical lateral distal femoral angle (aLDFA), mechanical lateral distal femoral angle (mLDFA), inclination of the femoral head angle (IFA), and femoral varus angle (FVA) were measured in the craniocaudal view of the radiographs and the frontal view of the CT images of the femur (▶Figure 3A–C) (20, 25, 26).

The anatomical caudal proximal femoral angle (aCdPFA), mechanical caudal

c Aquilion LB 16 Slice, Toshiba Medical Systems, Otawara, Japan
d AZE VirtualPlace, AZE Co., Ltd, Tokyo, Japan

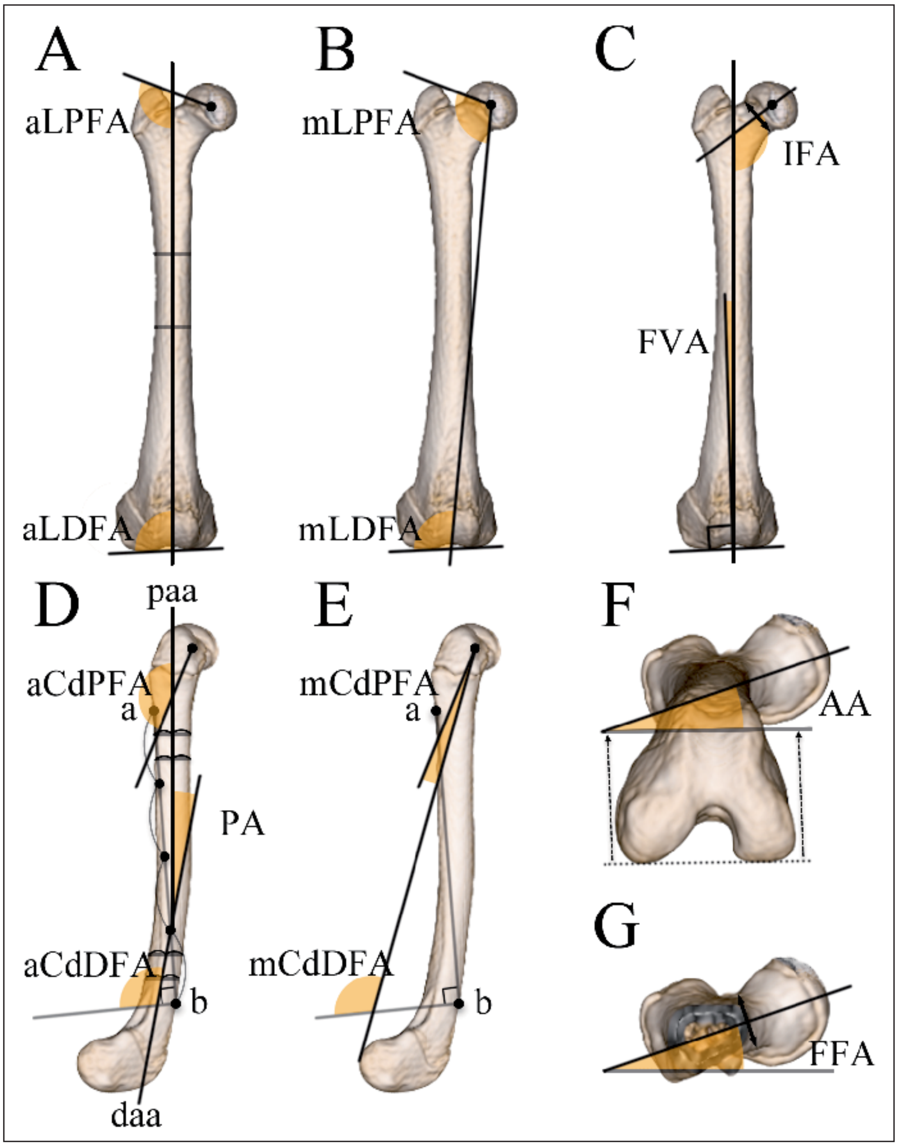

Figure 3 Measurement values for the femur. **A)** Anatomical lateral proximal femoral angle (aLPFA): the angle formed by the reference line and the proximal joint orientation line; anatomical lateral distal femoral angle (aLDFA): angle formed by the reference line and the distal joint orientation line. **B)** Mechanical lateral proximal femoral angle (mLPFA): angle formed by the mechanical axis and the proximal joint orientation line; mechanical lateral distal femoral angle (mLDFA): angle formed by the mechanical axis and the distal joint orientation line. **C)** Inclination of the femoral head angle (IFA): angle formed by the axis of femoral neck and the reference line; femoral varus angle (FVA): angle formed by the reference line and the line perpendicular to the distal joint orientation line. **D)** Anatomical caudal proximal femoral angle (aCdPFA): angle formed by the axis of femoral neck and proximal anatomical axis (paa); anatomical caudal distal femoral angle (aCdDFA): the angle formed by the distal anatomical axis (daa) and the line perpendicular to line a (lesser trochanter) through b (the limit of trochlea); procurvation angle (PA): the angle formed by paa and daa. **E)** Mechanical caudal proximal femoral angle (mCdPFA): angle formed by the axis of femoral neck and the mechanical axis, mechanical caudal distal femoral angle (mCdDFA): angle formed by the mechanical axis and the line perpendicular to the line a through b. **F)** Anteversion angle (AA): angle formed by the axis of the femoral neck and the transcondylar axis (dotted line). **G)** Frontal angle of the femoral neck (FFA): angle formed by the axis of the femoral neck and horizontal line.

proximal femoral angle (mCdPFA), anatomical caudal distal femoral angle (aCdDFA), and mechanical caudal distal femoral angle (mCdDFA) were measured in the mediolateral view of the radiographs or the lateral view of the CT images (▶ Figure 3D, E) (25, 27). We also defined the procurvation angle (PA) and recorded its value (▶ Figure 3D).

The anteversion angle (AA) was measured on the axial view of the CT image of the femur (▶ Figure 3F) (15, 18, 28-30). We also defined the frontal angle of the femoral neck (FFA) and measured it as shown in ▶ Figure 3G.

Tibia

The mechanical medial proximal tibial angle (mMPTA) and the mechanical medial distal tibial angle (mMDTA) were measured in the craniocaudal view of radiographs or the frontal view of CT images of the tibia (▶ Figure 4A) (25, 31).

The mechanical cranial proximal tibial angle (mCrPTA), mechanical cranial distal tibial angle (mCrDTA), tibial plateau angle (TPA), Z angle, and relative tibial tuberosity width (rTTW) were measured in the mediolateral view of radiographs of the tibia (25, 32, 33). On CT imaging, the mCrDTA was measured in the lateral view of the tibia (▶ Figure 4B), and the mCrPTA, TPA (▶ Figure 4C), Z angle, and rTTW (▶ Figure 4D) were investigated in the proximal lateral view of the tibia.

To evaluate torsion of the tibia, the tibial torsion angle (TTA) was calculated as described previously (▶ Figure 4E) (22, 24). Furthermore, in the axial view of the tibia, the ratio of the medial distance of the tibial tuberosity to the proximal tibial width (MDTT/PTW) was calculated to evaluate the medial displacement of the tibial tuberosity (▶ Figure 4F).

Patella

The length, width, and depth of the patella were measured on both radiographic and CT images. In addition, the volume of the patella was measured by CT, and the ratio of the patellar ligament length to the length of the patella (L:P ratio) was calculated to

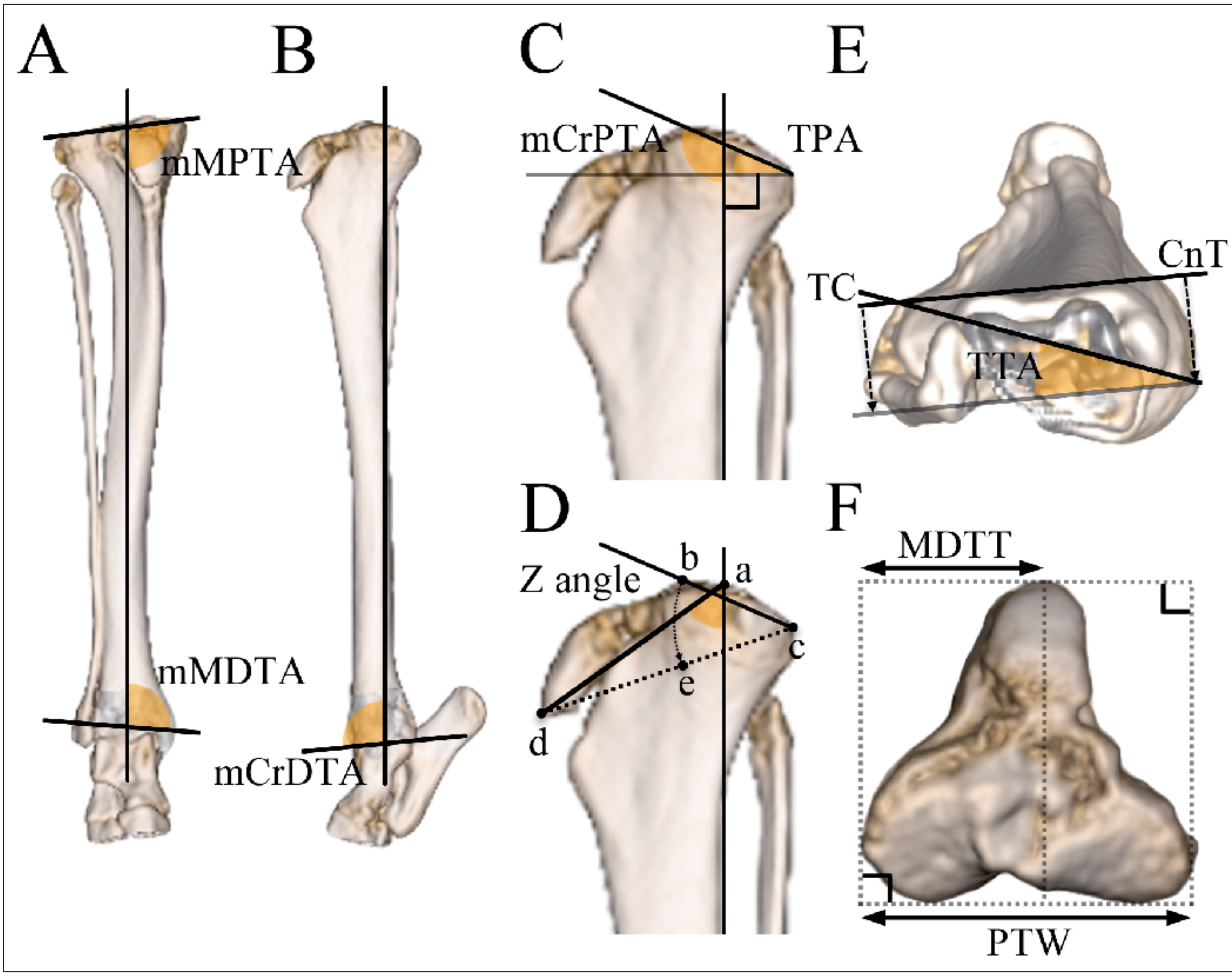

Figure 4 Measurement values for the tibia. **A)** Mechanical medial proximal tibial angle (mMPTA): angle formed by the reference line and the proximal joint orientation line; mechanical medial distal tibial angle (mMDTA): angle formed by the reference line and the distal joint orientation line. **B)** Mechanical cranial distal tibial angle (mCrDTA): angle formed by the reference line and the distal joint orientation line. **C)** Mechanical cranial proximal tibial angle (mCrPTA): angle formed by the reference line and the proximal joint orientation line; tibial plateau angle (TPA): angle formed by the proximal joint orientation line and the line perpendicular to the reference line. **D)** Z angle: angle formed by line a through d and the reference line; relative tibial tuberosity width (rTTW): ratio of line d through e to line c through e. **E)** Tibial torsion angle (TTA): angle formed by the transcondylar (TC) axis and the cranial tibial (CnT) axis. **F)** Proximal tibial width (PTW): width of the proximal tibia; medial distance of tibial tuberosity (MDTT): distance from the edge of the medial condyle of tibia to the tibial tuberosity. a: Mid-point of the medial and lateral intercondylar eminences, b: most cranial point of the tibial plateau, c: most caudal point of the tibial plateau, d: top of the tibial tuberosity, e: cross point of a circle with centre c and radius b through c.

evaluate the relationship between the vertical position of the patella and MPL (►Figure 5) (34).

Statistical analysis

Statistical analyses were performed using a data analysis software package[e]. Measurement values were expressed as the mean and standard deviation (SD). A one-way analysis of variance (ANOVA) was performed to compare groups with continuous data that were normally distributed according to the results of the D'Agostino-Pearson omnibus normality test. Tukey's multiple comparison was used as the post-hoc test. Unpaired t-tests were used to compare measurement values between radiographs and CT imaging. A p-value of <0.05 indicated statistical significance.

Results

Patients

Thirty-five hindlimbs of 23 Toy Poodles were evaluated during the study period. The mean age of these dogs was 1.1 ± 2.0 years (range: 3 months to 7 years), and the mean

e GraphPad Prism version 6.0 for Macintosh, GraphPad Software Inc., San Diego, CA, USA

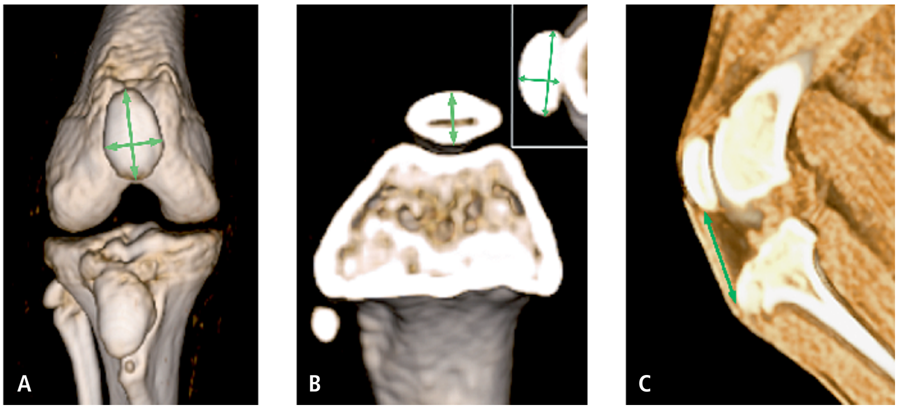

Figure 5 Measurement values for the patella. **A)** Length of the patella: longest dimension of the patella; width of the patella: widest dimension of the patella. **B)** Depth of the patella: the deepest dimension, perpendicular to the long axis of the patella. **C)** Length of the patellar ligament: distance from the point of origin of the patellar ligament on the distal aspect of the patella to its insertion on the proximal extent of the tibial tuberosity; L:P ratio: ratio of patellar ligament length to length of the patella.

body weight was 2.8 ± 1.4 kg (range: 1.35 to 6.38 kg). The dogs comprised six males (3 castrated) and 17 females (8 spayed). The hindlimbs with MPL were classified according to Singleton's grading system into grade 2 (n = 10), grade 4 (n = 10), and normal (n = 15). In the normal group, four dogs had one normal stifle and the contralateral stifles had medial (grade 1, n = 1; grade 4, n = 2) or lateral (grade 2, n = 1) patellar luxation.

Differences between imaging tools

When the morphology of the femur, tibia, and patella was evaluated using 3D CT imaging, all measurement values that were reported previously were reproduced and various bone deformities could be evaluated accurately. All measurement values of the femur could also be evaluated on radiographs, even when patellar luxation was severe. Conversely, not all measurement values of the tibia in the grade 4 group could be evaluated because of severe rotation deformity of the proximal tibia. The MDTT/PTW and the TTA could not be evaluated using radiographs.

Significant differences were found between imaging tools in the majority of the measurement values obtained from the frontal aspect of the femur (▶Table 1). No significant difference was identified between imaging tools in any of the measurements obtained from the lateral aspect of the femur. Among the values for the tibia that could be measured on both radiographs and CT, significant differences were

Table 1 Measurement values for the femur.

	Normal		Grade 2		Grade 4	
	Radiography	CT	Radiography	CT	Radiography	CT
aLPFA	106.6 ± 8.7^{*c}	119.5 ± 5.7^{*c}	107.6 ± 6.3$^{\dagger c}$	118.7 ± 4.4†	96.5 ± 8.4$^{\S ab}$	112.7 ± 6.8$^{\S a}$
mLPFA	102.1 ± 8.8^{*c}	113.6 ± 6.1*	101.5 ± 7.7†	113.1 ± 3.9†	93.8 ± 5.5$^{\S a}$	109.7 ± 6.4§
aLDFA	94.4 ± 4.1^{*c}	90.3 ± 2.8^{*c}	94.3 ± 4.8$^{\dagger c}$	89.5 ± 3.8$^{\dagger c}$	110.5 ± 8.5^{b}	108.1 ± 8.0^{ab}
mLDFA	99.1 ± 3.1^{*c}	96.2 ± 2.5^{*c}	99.3 ± 3.9$^{\dagger c}$	95.0 ± 3.6$^{\dagger c}$	113.3 ± 5.3^{ab}	111.1 ± 6.9^{ab}
FVA	4.4 ± 4.1^{*c}	0.3 ± 2.8^{*c}	4.3 ± 4.8$^{\dagger c}$	-0.6 ± 3.8$^{\dagger c}$	20.5 ± 8.5^{ab}	18.1 ± 8.0^{ab}
IFA	127.7 ± 6.3*	116.8 ± 6.1*	124.6 ± 7.1†	118.0 ± 6.8†	125.0 ± 6.1	118.3 ± 9.3
PA	12.7 ± 4.1	11.2 ± 5.2	12.7 ± 7.1	11.1 ± 5.4	14.2 ± 7.3	15.8 ± 6.9
aCdPFA	157.3 ± 7.7	153.3 ± 5.1	153.3 ± 8.0	151.6 ± 6.0	152.5 ± 11.3	151.7 ± 5.6
mCdPFA	7.5 ± 5.9	9.6 ± 5.5	10.6 ± 7.5	11.3 ± 5.9	13.4 ± 8.8	10.4 ± 6.2
aCdDFA	104.3 ± 2.1	102.9 ± 3.2	104.5 ± 5.6	102.6 ± 3.5	105.6 ± 6.9	104.7 ± 5.7
mCdDFA	107.8 ± 1.9	108.4 ± 1.7	107.0 ± 3.7	107.5 ± 2.6	107.5 ± 1.8	107.0 ± 2.7
AA	NE	19.8 ± 4.6^{c}	NE	16.6 ± 4.8^{c}	NE	9.6 ± 5.2^{ab}
FFA	NE	20.8 ± 4.1	NE	21.7 ± 4.9	NE	19.3 ± 7.6

$^{*, \dagger, \S}$: Mean values in the same row that have the same superscript reference symbols are significantly different between imaging tools ($p < 0.05$) (*Normal; †Grade 2; §Grade 4). $^{a, b, c}$: Within the same row, mean values obtained from the same imaging tool that have superscript lower case letters are significantly different between MPL grade groups ($p < 0.05$) (^{a} vs. Normal; ^{b} vs. Grade 2; ^{c} vs. Grade 4). aLPFA = anatomical lateral proximal femoral angle; mLPFA = mechanical LPFA; aLDFA = anatomical lateral distal femoral angle; mLDFA = mechanical LDFA; FVA = femoral varus angle; IFA = inclination of the femoral head angle; PA = procurvation angle; aCdPFA = anatomical caudal proximal femoral angle; mCdPFA = mechanical CdPFA; aCdDFA = anatomical caudal distal femoral angle; mCdDFA = mechanical CdDFA; AA = anteversion angle; FFA = frontal angle of the femoral neck; NE = not evaluated.

Table 2 Measurement values for the tibia.

	Normal		Grade 2		Grade 4	
	Radiography	CT	Radiography	CT	Radiography	CT
mMPTA	94.4 ± 3.8	94.8 ± 2.1	96.9 ± 3.5	94.7 ± 1.7	NE	94.5 ± 4.4
mMDTA	96.5 ± 2.3	96.5 ± 4.1	94.2 ± 4.4	95.2 ± 2.4	NE	98.5 ± 4.1
mCrPTA	117.5 ± 4.7*	111.3 ± 3.3*	118.4 ± 5.3†	111.2 ± 3.4†	NE	112.7 ± 4.2
mCrDTA	91.0 ± 4.6*	98.5 ± 3.8*	88.8 ± 2.0†	99.2 ± 3.1†	NE	98.6 ± 6.4
TPA	27.6 ± 4.7	21.3 ± 3.3	28.4 ± 5.3	21.2 ± 3.4	NE	22.7 ± 4.2
Z angle	63.8 ± 5.2	65.7 ± 4.6	64.5 ± 3.9	66.2 ± 3.8	NE	67.2 ± 5.8
rTTW	0.86 ± 0.08	0.74 ± 0.09	0.91 ± 0.15	0.73 ± 0.13	NE	0.76 ± 0.10
TTA	NE	11.3 ± 4.3[c]	NE	13.0 ± 7.9[c]	NE	32.8 ± 7.9[ab]
MDTT/PTW	NE	0.52 ± 0.04[c]	NE	0.51 ± 0.05[c]	NE	0.43 ± 0.05[ab]

*, †, §: Mean values in the same row that have same superscript reference symbols are significantly different between imaging tools ($p < 0.05$) (*Normal; †Grade 2; §Grade 4). a, b, c: Within the same row, mean values obtained from the same imaging tool that have superscript lower cases are significantly different between MPL grade groups ($p < 0.05$) (a vs. Normal; b vs. Grade 2; c vs. Grade 4). mMPTA = mechanical medial proximal tibial angle; mMDTA = mechanical medial distal tibial angle; mCrPTA = mechanical cranial proximal tibial angle; mCrDTA = mechanical cranial distal tibial angle; TPA = tibial plateau angle; rTTW = relative tibial tuberosity width; TTA = tibial torsion angle; MDTT/PTW = ratio of the medial distance of the tibial tuberosity to the proximal tibial width; NE = not evaluated.

observed between imaging tools (▶Table 2). In the measurement of the patella, no significant difference was found between imaging tools (▶Table 3).

Femur

The aLDFA, mLDFA, and FVA, which are the index for varus deformity in the grade 4 group, were significantly higher than those in the other groups on both radiographs and CT imaging. In addition, the AA in the grade 4 group was significantly lower than that in the other groups. No significant difference was found in the other measurement values among the groups, including IFA, aCdPFA, mCdPFA, aCdDFA, mCdDFA, PA, and FFA (▶Table 1, ▶Figure 6).

Tibia

The TTA in the grade 4 group was significantly higher than that in the other groups (▶Table 2). In addition, the MDTT/PTW in the grade 4 group was significantly lower than that in the other groups. By contrast, no significant difference was identified among the groups in the other values measured on CT, including mMPTA, mMDTA, mCrPTA, TPA, mCrDTA, Z angle, and rTTW. In addition, no significant difference was observed among the groups in any of the measurements obtained from radiographs (▶Figure 7).

Patella

No significant differences were found among groups in the L:P ratio by either radiography or CT (▶Table 3). The patellar width obtained from radiographs in the grade 4 group was significantly less than that in the normal group. In addition, the patellar length and depth obtained by both radiography and CT in the grade 4 group were significantly less than those in the normal group, and the volume of the patella measured by CT in the grade 4 group was significantly lower than that of the normal group.

Discussion

Most of the bone morphology of the femur could be evaluated by radiography in all groups. However, measurements of the tibia could not be obtained by radiography when the internal torsion of the proximal tibia was severe. In contrast, all measurements were evaluated accurately on CT using 3D volume image reconstruction, even when severe bone deformities were present.

Table 3 Measurement values for the patella.

	Normal		Grade 2		Grade 4	
	Radiography	CT	Radiography	CT	Radiography	CT
Length	10.6 ± 1.7[c]	10.6 ± 1.6[c]	9.1 ± 1.0[a]	9.2 ± 0.9[a]	9.2 ± 1.3[a]	9.2 ± 1.2[a]
Width	6.7 ± 1.3[c]	6.8 ± 1.2	5.9 ± 1.1	5.9 ± 1.0	5.3 ± 1.2[a]	5.7 ± 1.0
Depth	4.1 ± 0.6[c]	4.5 ± 0.5[c]	3.6 ± 0.5	3.8 ± 0.5[a]	3.2 ± 0.9[a]	3.3 ± 0.6[a]
Volume	NE	0.22 ± 0.08[c]	NE	0.15 ± 0.06	NE	0.13 ± 0.07[a]
L:P ratio	1.74 ± 0.17	1.77 ± 0.19	1.75 ± 0.14	1.71 ± 0.10	1.66 ± 0.24	1.60 ± 0.27

a, b, c: Within the same row, mean values obtained from same imaging tool that have superscript lower cases are significantly different between MPL grade groups ($p < 0.05$) (a vs. Normal; b vs. Grade 2; c vs. Grade 4). L:P ratio = ratio of the patellar ligament length to the length of the patella; NE = not evaluated.

In this study, there were significant differences between imaging tools with regard to measurement values obtained from the femur, tibia, and patella. The inability to accurately determine femoral varus and tibial torsion on radiographs was well established by previous studies (22, 35). In particular, femoral morphology and measurement values are more likely to vary according to the angle formed by the bone and the radiographic table. In addition, bisection of the fabellae has been shown to not be an accurate determinant of craniocaudal femoral projection (36). In contrast, the superiority of CT is well established (18). Radiographs have been traditionally used for corrective osteotomy in dogs with MPL. However, not all dogs with bone deformities are evaluated using CT in small-animal practice (35). Therefore, we compared the differences in various parameters between imaging tools.

Most previous studies examining bone morphology associated with MPL have included various breeds (11, 15, 16, 18). To decrease the variability associated with anatomical differences among breeds, it was preferable in the present study to focus on a single breed. Therefore, we employed only the Toy Poodle, which is known to have a breed predilection for MPL (4–7). In addition, to the best of our knowledge, there have not been any studies evaluating the bone morphology of both the femur and tibia comprehensively in dogs with grade 4 MPL. Therefore, for the first time, we evaluated the bone morphology of both the femur and tibia in Toy Poodles with severe bone deformities, including grade 4 MPL, using 3D CT imaging; we also investigated the relationship between the severity of MPL and bone deformities.

It has been reported that varus deformity of the distal one-third of the femur occurs as MPL severity grade increases (1-3, 10). In the present study, the parameters of the aLDFA, mLDFA, and FVA obtained from 3D CT imaging in the grade 2 group were not significantly different from those of the normal group, which was similar to previous results (11). However, these values were significantly higher in the grade 4 group than in the other groups. These results indicate that significant femoral varus deformity was present in the grade 4 group. Persistent pressure on the distal femoral physis generated by medial malalignment of the quadriceps muscles associated with MPL at birth or early in life may aggravate femoral deformities (1, 10). Our findings concerning the grade 4 group may support this hypothesis.

Coxa vara and retroversion of the femoral neck are important factors that have been associated with MPL (3, 10, 13, 19, 37, 38). In the present study, the IFA measured by 3D CT imaging was not significantly different among the groups, which suggests that coxa vara was not associated with MPL of any severity, as previously reported using radiographs (11, 12, 16). The AA is used as the angle for evaluation of the inclination of the femoral neck in the axial view of the femur (29). In the present study, the AA measured by 3D CT imaging in the grade 4 group was significantly lower than that in the other groups. The relationship between MPL and AA was controversial in previous studies (13, 38). Recent studies have demonstrated that the AA can be evaluated accurately by CT or magnetic resonance imaging (MRI). However, retroversion of the femoral neck in dogs with MPL was not confirmed in those studies (13, 15). The AA measured from radiographs is highly susceptible to positional artefacts and is influenced by external torsion of the distal femur and hypoplasia of the medial condyle (14, 39). Therefore, to evaluate the inclination of the femoral neck to the axis of the femur accurately, we introduced the FFA in the present study, as measured by 3D CT imaging. No significant differences in FFA were found among groups. These results suggest that the inclination of the femoral neck is not associated with the severity of MPL.

Previous studies have reported that medial displacement of the tibial tuberos-

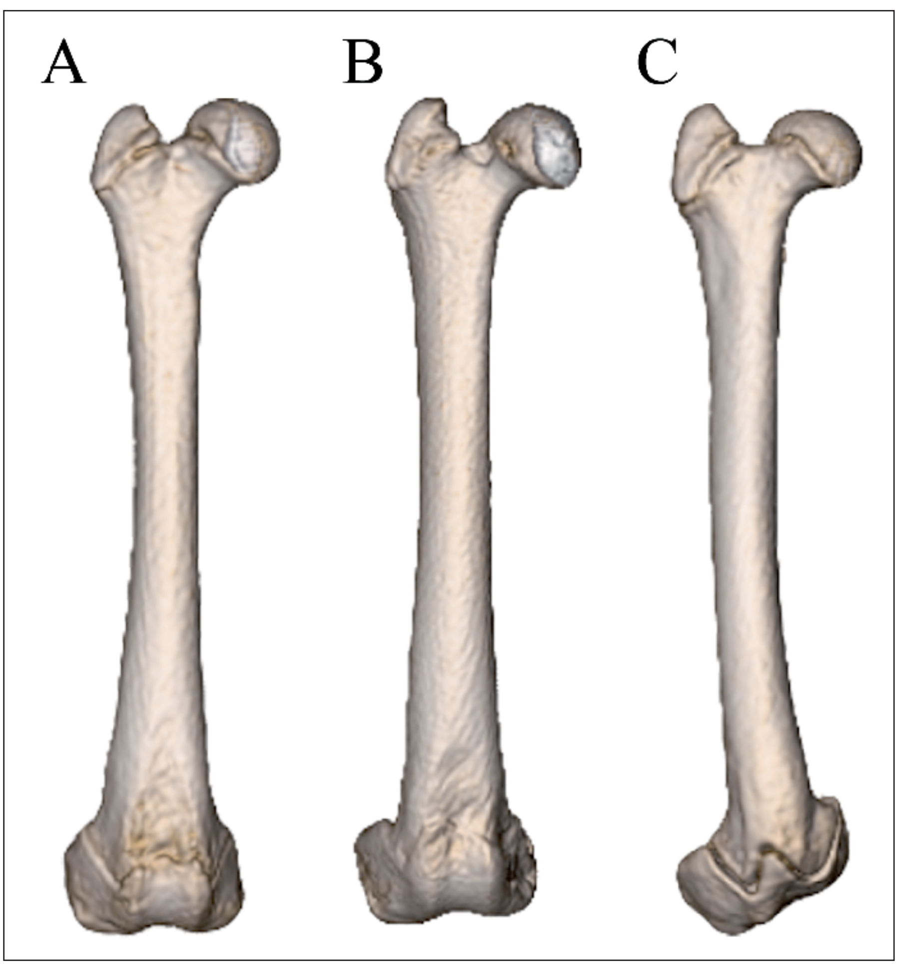

Figure 6 Frontal views of the femur for each medial patellar luxation grade obtained by three-dimensional computed tomography. **A)** Normal, **B)** Grade 2, **C)** Grade 4.

ity, internal torsion of the proximal tibia, and valgus deformity of the proximal tibia occur as the MPL severity increases (1-3, 10). In the present study, the MDTT/PTW, which is an index of medial displacement of tibial tuberosity, was significantly lower in the grade 4 group than in the other groups. In addition, the TTA was significantly higher in the grade 4 group than in the other groups. No significant differences in these values were identified between the normal and grade 2 groups. These results suggest that medial displacement of the tibial tuberosity and internal torsion of the proximal tibia occur in Toy Poodles with severe MPL. To the best of our knowledge, the present study is the first report on objective evaluation of tibial deformities associated with severe internal torsion of the proximal site of MPL. However, the mMPTA and mMDTA were not significantly different among the groups with regard to the values obtained by 3D CT. In contrast to previous studies, this indicates a lack of tibial valgus deformity associated with severe MPL (16). In addition, in the present study, there were no significant differences among the groups in mCrPTA, TPA, mCrDTA, Z angle, and rTTW obtained by 3D CT. Therefore, longitudinal malposition of the tibial tuberosity, variation of tibial plateau angle, and procurvation or recurvation of the tibia did not occur in any MPL grades.

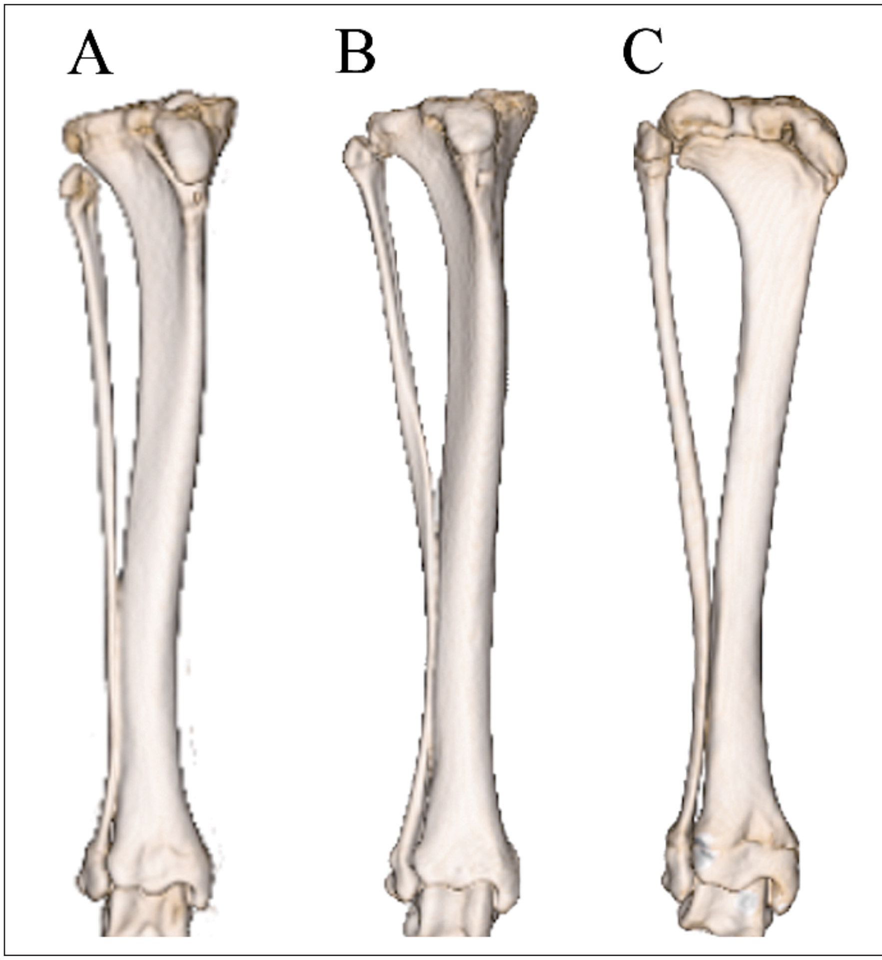

Figure 7 Frontal views of the tibia for each medial patellar luxation grade obtained by three-dimensional computed tomographic imaging. **A)** Normal, **B)** Grade 2, **C)** Grade 4.

To the best of our knowledge, there has not been any other report of a study investigating variation of patellar morphology according to MPL grade. In the present study, the length, depth, and volume of the patella measured by 3D CT in the grade 4 group were significantly lower than those in the normal group. These findings suggest that improper articulation of the patella within the trochlear groove leads to patellar hypoplasia. A previous study demonstrated that patella alta was associated with MPL in large-breed dogs (40). We investigated the relationship between the vertical position of the patella and MPL according to L:P ratio obtained by 3D CT, but did not find a significant difference among groups in the L:P ratio. This result indicates that the severity of MPL is not associated with patella alta in Toy Poodles.

In the previous studies, the relative role of soft tissue abnormalities and bone deformities in the pathogenesis of MPL was unclear. Surgical treatment has traditionally focused upon skeletal reconstruction of the shallow trochlear sulcus and medial displacement of the tibial tuberosity (20). However, from the results of the present study, a comprehensive evaluation of the femur and tibia by 3D CT may indicate that these bones are deformed toward the line connecting the origin and insertion of the quadriceps muscles. Therefore, bone deformities associated with severe MPL may be caused by persistent traction resulting from malalignment of the quadriceps muscles. For these reasons, surgical treatments for MPL should be performed before severe bone deformities occur. In addition, the results of the present study may be helpful if corrective osteotomy is considered in Toy Poodles with severe MPL.

In the present study, torsion of the femur, hypoplasia of the femoral condyles, and depth of the trochlear groove were not evaluated objectively because the appropriate landmarks to investigate these morphologies could not be established. Further investigations to establish appropriate measurement methods are needed. In the present study, hindlimbs were simply classified according to the Singleton grading system. Ideally, dogs with bilaterally normal hindlimbs should be evaluated as controls because subclinical bone deformities may exist in the unaffected legs of affected dogs. Bone morphology in grade 1 and 3 MPL groups was not evaluated because the sample size was small in these groups during the investigation period. The measurement values in these groups may increase the understanding of bone deformities associated with MPL. It is also necessary to investigate the effect of muscles and tendons on bone deformities during growth.

In conclusion, this study demonstrated significant differences between radiography and 3D CT imaging in the evaluation of the bone morphology of the femur, tibia, and patella in dogs with severe MPL. Toy Poodles with severe MPL (grade 4) had significant femoral varus deformity, medial displacement of the tibial tuberosity, internal torsion of the proximal tibia, and hypoplasia of the patella. Toy Poodles with grade 2 MPL had no significant bone deformities compared to normal dogs. These results will be helpful for understanding the pathophysiology of MPL.

Conflicts of interest

There are no conflicts to declare for any of the authors in relation to this paper.

References

1. Schulz K. Diseases of the Joints. In: Fossum TW, editor. Small Animal Surgery. 3rd ed. St Louis: Mosby Elsevier; 2002. Pg. 1143–1315.
2. Vasseur PB. Stifle joint. In: Vasseur PB, editor. Textbook of Small Animal Surgery. 3rd ed. Philadelphia: Saunders; 2003. Pg. 2090–2132.
3. Piermattei DL, Flo GL. The stifle joint. In: Brinker WO, Piermattei DL, Flo GL, editors. Handbook of Small Animal Orthopedics and Fracture Repair. 4th ed. Philadelphia: Saunders; 2006. Pg. 562–582.
4. Hodgman SF. Abnormalities and defects in pedigree dogs–I. An investigation into the existence of abnormalities in pedigree dogs in the British Isles. J Small Anim Pract 1963; 4: 447–456.
5. Priester WA. Sex, size, and breed as risk factors in canine patellar luxation. J Am Vet Med Assoc 1972; 160: 740–742.
6. Hayes AG, Randy JB, Hunderford LL. Frequency and distribution of medial and lateral patellar luxation in dogs: 124 cases (1982–1992). J Am Vet Med Assoc 1994; 205: 716–720.
7. LaFond E, Breur GJ, Austin CC. Breed susceptibility for developmental orthopedic diseases in dogs. J Am Anim Hosp Assoc 2002; 38: 467–477.
8. Alam MR, Lee JI, Kang HS, et al. Frequency and distribution of patellar luxation in dogs. 134 cases (2000 to 2005). Vet Comp Orthop Traumatol 2007; 20: 59–64.
9. Swiderski JK, Palmer RH. Long-term outcome of distal femoral osteotomy for treatment of combined distal femoral varus and medial patellar luxation: 12 cases (1999–2004). J Am Vet Med Assoc. 2007; 231: 1070–1075.
10. Hulse DA. Pathophysiology and management of medial patellar luxation in the dog. Vet Med Small Anim Clin 1981; 76: 43–51.
11. Mortari AC, Rahal SC, Vulcano LC, et al. Use of radiographic measurements in the evaluation of dogs with medial patellar luxation. Can Vet J 2009; 50: 1064–1068.
12. Soparat C, Wangdee C, Chuthatep S, et al. Radiographic measurement for femoral varus in Pomeranian dogs with and without medial patellar luxation. Vet Comp Orthop Traumatol 2012; 25: 197–201.
13. Kaiser S, Cornely D, Golder W, et al. The correlation of canine patellar luxation and the anteversion angle as measured using magnetic resonance images. Vet Radiol Ultrasound 2001; 42: 113–118.
14. Roch SP, Gemmill TJ. Treatment of medial patellar luxation by femoral closing wedge ostectomy using a distal femoral plate in four dogs. J Small Anim Pract 2008; 49: 152–158.
15. Towle HA, Griffon DJ, Thomas MW, et al. Pre- and postoperative radiographic and computed tomographic evaluation of dogs with medial patellar luxation. Vet Surg 2005; 34: 265–272.
16. Bound N, Zakai D, Butterworth S, et al. The prevalence of canine patellar luxation in three centres. Vet Comp Orthop Traumatol 2009; 22: 32–37.
17. Fitzpatrick CL, Krotscheck U, Thompson MS, et al. Evaluation of tibial torsion in Yorkshire Terriers with and without medial patellar luxation. Vet Surg 2012; 41: 966–972.
18. Barnes DM, Anderson AA, Frost C, et al. Repeatability and reproducibility of measurements of femoral and tibial alignment using computed tomography multiplanar reconstructions. Vet Surg 2015; 44: 85–93.
19. Singleton WB. The surgical correction of stifle deformities in the dog. J Small Anim Pract 1969; 10: 59–69.
20. Swiderski JK, Radecki SV, Park RD, et al. Comparison of radiographic and anatomic femoral varus angle measurements in normal dogs. Vet Surg 2008; 37: 43–48.
21. Bardet JF, Rudy RL, Hohn RB. Measurement of femoral torsion in dogs using a biplanar method. Vet Surg 1983; 12: 1–6.
22. Apelt D, Kowaleski MP, Dyce J. Comparison of computed tomographic and standard radiographic determination of tibial torsion in the dog. Vet Surg 2005; 34: 457–462.
23. Dismukes DI, Tomlinson JL, Fox DB, et al. Radiographic measurement of canine tibial angles in the sagittal plane. Vet Surg 2008; 37: 300–305.
24. Aper R, Kowaleski MP, Apelt D, et al. Computed tomographic determination of tibial torsion in the dog. Vet Radiol Ultrasound 2005; 46: 187–191.
25. Paley D. Normal lower limb alignment and joint orientation. In: Principles of Deformity Correction. Berlin, Germany: Springer-Verlag; 2003; 1–18.
26. Hauptman J. The angle of inclination of the canine femoral head and neck. Vet Surg 1979; 8: 74–77.
27. Petazzoni M. Hind limb alignment in the dog to treat patellar luxation: a retrospective study of 39 cases (2001–2005). 13th Conference of the European Society of Veterinary Orthopaedics and Traumatology; 2006 September 7–10; Munich, Germany. pg. 263.
28. Dudley RM, Kowaleski MP, Drost WT, et al. Radiographic and computed tomographic determination of femoral varus and torsion in the dog. Vet Radiol Ultrasound 2006; 47: 546–552.
29. Nunamaker DM, Beiry DN, Newton CD. Femoral neck anteversion in the dog: its radiographic measurement. Vet Radiol Ultrasound 1973; 14: 45–48.
30. Mostafa AA, Griffon DJ, Thomas MW, et al. Radiographic evaluation of femoral torsion and correlation with computed tomographic techniques in Labrador Retrievers with and without cranial cruciate ligament disease. Vet Surg 2014; 43: 534–541.
31. Dismukes DI, Tomlinson JL, Fox DB, et al. Radiographic measurement of the proximal and distal mechanical joint angles in the canine tibia. Vet Surg 2007; 36: 699–704.
32. Fettig AA, Rand WM, Sato AF, et al. Observer variability of tibial plateau slope measurement in 40 dogs with cranial cruciate ligament-deficient stifle joints. Vet Surg 2003; 32: 471–478.
33. Vedrine B, Guillemot A, Fontaine D, et al. Comparative anatomy of the proximal tibia in healthy Labrador retrievers and Yorkshire terriers. Vet Comp Orthop Traumatol 2008; 26: 266–270.
34. Mostafa AA, Griffon DJ, Thomas MW, et al. Proximodistal alignment of the canine patella: radiographic evaluation and association with medial and lateral patellar luxation. Vet Surg 2008; 37: 201–211.
35. Swiderski JK, Palmer RH. Long-term outcome of distal femoral osteotomy for treatment of combined distal femoral varus and medial patellar luxation: 12 cases (1999–2004). J Am Vet Med Assoc 2007; 231: 1070–1075.
36. Aiken M, Barnes D. Are the fabellae bisected by the femoral cortices in a true craniocaudal pelvic limb radiograph? J Small Anim Pract 2014; 55: 465–470.
37. Roush JK. Canine patellar luxation. Vet Clin North Am Small Anim Pract 1993; 23: 855–868.
38. Campbell JR, Pond MJ. The canine stifle joint II. Medial luxation of the patella: An assessment of lateral capsular overlap and more radical surgery. J Small Anim Pract 1972; 13: 11–18.
39. Kowaleski MP. Patellar luxation – preoperative evaluation and surgical planning for femoral corrective osteotomy. 13th Conference of the European Society of Veterinary Orthopaedics and Traumatology; 2006 September 7–10; Munich, Germany. pg. 87–90.
40. Johnson AL, Broaddus KD, Hauptman JG, et al. Vertical patellar position in large-breed dogs with clinically normal stifles and large-breed dogs with medial patellar luxation. Vet Surg 2006; 35: 78–81.